

# Linear-in-T resistivity from semi-holographic non-Fermi liquid models

Benoît Douçot\*

*Laboratoire de Physique Théorique et Hautes Energies,  
Sorbonne Université and CNRS UMR 7589, 4 place Jussieu, 75252 Paris Cedex 05, France*

Ayan Mukhopadhyay†

*Department of Physics, Indian Institute of Technology Madras, Chennai 600036, India*

Giuseppe Policastro‡

*Laboratoire de Physique de l'Ecole Normale Supérieure, CNRS, Université PSL,  
Sorbonne Universités, Université Pierre et Marie Curie, 24 rue Lhomond, 75005 Paris, France*

Sutapa Samanta§

*School of Physical Sciences, Indian Association for the Cultivation of Science, Jadavpur, Kolkata 700032, India*

(Dated: March 19, 2022)

We construct a semi-holographic effective theory in which the electron of a two-dimensional band hybridizes with a fermionic operator of a critical holographic sector, while also interacting with other bands that preserve quasiparticle characteristics. Besides the scaling dimension  $\nu$  of the fermionic operator in the holographic sector, the effective theory has two dimensionless couplings  $\alpha$  and  $\gamma$  determining the holographic and Fermi-liquid-type contributions to the self-energy respectively. We find that irrespective of the choice of the holographic critical sector, there exists a ratio of the effective couplings for which we obtain linear-in-T resistivity for a wide range of temperatures. This scaling persists to arbitrarily low temperatures when  $\nu$  approaches unity in which limit we obtain a marginal Fermi liquid with a specific temperature dependence of the self-energy.

## INTRODUCTION

The measurement of the spectral function via ARPES has given us key insights into the nature of elementary constituents in strongly correlated electronic systems which do not admit quasiparticle description, and which also demonstrate a rich variety of novel superconducting, metallic and insulating phases [1–3]. Phenomenological approaches to model strange metallic behavior have considered spectral functions with the following properties: (i) particle-hole asymmetry, (ii) semi-locality (i.e. very mild dependence on the momentum in the direction normal to the Fermi surface), and (iii) non-trivial scaling exponent with the frequency [4–6]. Such features are extremely challenging to obtain from a first principle approach.

It is quite remarkable that spectral functions with these properties arise in holographic theories at finite density; the infrared behavior is described by a Dirac fermion in the near-horizon  $AdS_2 \times R^2$  geometry of the black brane dual to the critical sector [7–12] concretely realizing the scenario of *deconfined criticality* [13]. Although such theories are essentially gauge theories and the microscopic description is possibly not relevant for material physics, the infrared fixed point with novel scaling behavior at finite density could be universal in a suitable large  $N$  limit and thus could provide a first principle realization of emergent non-Fermi liquid behavior.

The holographic approach allows one to dispense with the notion of quasiparticles, which are replaced by the

modes of the underlying (emergent) infrared conformal field theory, and this can be very useful to provide a unified picture of transport phenomena [14]. At the same time, this makes it difficult to understand what are the effective microscopic degrees of freedom of the system. In [15–20] it has been argued that in order to describe the strange metals, it is crucial to consider the effects of intermediate scale physics, especially that of the upper Hubbard band, on the critical sector – necessitating an approach that is often called *Mottness*. Such effects cannot be reliably modeled by a purely holographic approach. Bottom-up models [21–28] can holographically engineer a quantum critical sector that can reproduce the scaling of resistivity, Hall angle, etc with temperature but typically only in the low temperature regime (unless further contrived [29]).

Based on the key insights provided by Faulkner and Polchinski [30], a semi-holographic effective theory was proposed in [31] and further studied in [32]. The proposal of Faulkner and Polchinski was to retain only the infrared part of the holographic sector (i.e. the near horizon geometry) and allow linear hybridization of some of the bands on the lattice with the bulk holographic fermions; this results in a Fermi surface with low frequency behavior determined by the holographic critical sector, in particular by the scaling exponent  $\nu$  of the holographic fermion. In [31], it was shown that if one introduces short-range interactions among the lattice fermions and also more general mutual interactions between the lattice fermions and the holographic fermions with a spe-

cific form of large  $N$  scaling (see below), the low frequency behavior at the Fermi surface remains unaffected leading to the notion of a *generalized quasiparticle*. The density-density correlations and the case of Coulombic interactions was analyzed in [32]. In particular, it was found that in presence of a frequency cutoff, the semi-holographic theory exhibits well-defined collective excitations within the continuum above a certain momentum threshold and at reasonably low frequencies. It was speculated that these plasmonic excitations may provide a realization of the mid-infrared scenario for superconductivity proposed by Leggett [33, 34].

In this work, we address a key issue in this semi-holographic approach by achieving a natural UV completion that interpolates between non-Fermi liquid behavior at low frequencies/temperatures and Fermi liquid behavior at high frequencies/temperatures. The completion does not alter the generalized quasiparticle on the Fermi surface and is also insensitive to microscopic lattice effects. Such a scenario leads to an effective theory sharing some features with Mottness. Our construction is rather simple and is based on the assumption that the two-dimensional band of interest, in addition to hybridizing with the infrared critical sector, also interacts with other bands which have conventional quasiparticle behavior. We can engineer the interactions in a way that involves only two effective couplings. Because the theory is UV complete, observables are well-defined without the need of an ad hoc frequency cutoff as employed in [32], however we do reproduce the results of the latter work qualitatively and extend them to finite temperatures.

In this letter we use the model described above to compute the dc conductivity at finite temperature. Our main result is that we observe a linear-in-T resistivity for a wide range of temperatures when the scaling dimension  $\nu > \sim 0.67$ . For  $\nu \approx 2/3$ , as for instance, this linear scaling regime extends from  $0.3E_F$  to about  $20 - 40E_F$  when the couplings are small, but when  $\nu \approx 1$  it holds at arbitrary low temperatures also. Crucially, in our semi-holographic approach where we include perturbative degrees of freedom, we are able to obtain the linear-in-T resistivity *irrespective* of the critical sector (for a wide range of  $\nu$ ) as long as the ratio of the two effective couplings is optimal. Although the range of temperatures where this scaling is valid depends on  $\nu$ , it is typically very wide.

## A SIMPLE EFFECTIVE THEORY

We propose a simple effective theory based on a single band of electrons localized on a two-dimensional plane.

The starting point is the model studied in [31, 32]. It includes the creation and annihilation operators for the electrons in the band  $c^\dagger(\mathbf{k})$ ,  $c(\mathbf{k})$  which are hybridized linearly with a fermionic operator  $\chi_{CFT}(\mathbf{k})$  ( $\chi_{CFT}^\dagger(\mathbf{k})$ ) in

the critical sector described by a holographic  $AdS_2 \times R^2$  dual geometry. Crucially this band has no direct self-interactions because of a large- $N$  limit discussed in [31] in which the self interactions of the *bath* critical sector (an infrared conformal field theory (IR-CFT)) scale quadratically as  $N^2$  while the hybridization coefficient scales linearly with  $N$ . The backreaction of the metric is suppressed in this limit but the self-energy of the two-dimensional band receives an  $\mathcal{O}(N^0)$  correction in the form of a holographic fermionic propagator destroying its quasi-particle nature. It has been shown in [31] that the leading low-frequency behavior at the Fermi surface is unaltered as long as we introduce further interactions like  $c\chi^3$  which are linear in  $c(\mathbf{k})$  and  $c^\dagger(\mathbf{k})$ , and scale at most linearly with  $N$ . In this sense, the semi-holographic theory of this band creates a *generalized quasiparticle*.

One major problem with this version of the semi-holographic theory is that the UV behavior is not regular; one manifestation of this is the fact that the real part of the density-density correlation function (a.k.a the Lindhard function) is negative for all frequencies, unless we impose an artificial frequency cutoff as in [32]. However, we expect the high energy behavior of the theory to be more conventional with the real part of the Lindhard function being positive definite at high frequencies. It is therefore pertinent to look for a modification of this theory in which the conventional UV behavior is automatically obtained, without the need of a cut-off, and without altering the leading low-frequency non-Fermi liquid behavior resulting from the hybridization with the holographic bulk fermion.

Such a modification can be achieved if we assume that the two-dimensional band couples linearly with other bands which preserve their (Landau) quasiparticle characteristics. Denoting the creation (annihilation) operators of one-particle states in these bands as  $f_i^\dagger$  ( $f_i$ ) we allow only interactions of the type  $cf^3$ ,  $cf^5$ ,  $\dots$ . We thus consider the following Hamiltonian

$$\begin{aligned} \hat{H} = & \sum_{\mathbf{k}} \epsilon(\mathbf{k}) c^\dagger(\mathbf{k}) c(\mathbf{k}) + N \sum_{\mathbf{k}} (g(\mathbf{k}) c^\dagger(\mathbf{k}) \chi_{CFT}(\mathbf{k}) + c.c.) \\ & + N^2 \hat{H}_{IR-CFT} + \sum_{i,j,k} \left( \lambda_{ijk, \mathbf{k}_1, \mathbf{k}_2, \mathbf{k}_3} \right. \\ & \left. c^\dagger(\mathbf{k}_1) f_i(\mathbf{k}_2) f_j^\dagger(\mathbf{k}_3) f_k(\mathbf{k}_1 - \mathbf{k}_2 + \mathbf{k}_3) + c.c. \right) + \dots \end{aligned}$$

At leading order in the coupling  $\lambda$ , the  $c$ -fermions cannot run in the loops. This leads to factorization of the self-energy of the  $c$ -band into two parts, namely the contribution from the holographic propagator and a Fermi-liquid type self-energy term.

In this effective theory the finite-temperature retarded Green's function of the  $c$ -band should take the form

$$\begin{aligned} G(\omega, \mathbf{k}) = & \left( \omega + i\tilde{\gamma}(\omega^2 + \pi^2 T^2) + \tilde{\alpha} \mathcal{G}(\omega) \right. \\ & \left. - \left( \frac{\mathbf{k}^2}{2m} - \frac{k_F^2}{2m} \right) \right)^{-1} \end{aligned} \quad (1)$$

with  $\tilde{\gamma} = \mathcal{O}(\lambda^2)$  being the coefficient of the Fermi-liquid type self-energy term,  $\tilde{\alpha} = \mathcal{O}(|g|^2)$  and  $\mathcal{G}(\omega)$  is the contribution of the holographic sector on the Fermi surface with the form [10, 35]

$$\mathcal{G}(\omega, T) = e^{i(\phi + \pi\nu/2)} (2\pi T)^\nu \frac{\Gamma(\frac{1}{2} + \frac{\nu}{2} - i\frac{\omega}{2\pi T})}{\Gamma(\frac{1}{2} - \frac{\nu}{2} - i\frac{\omega}{2\pi T})}. \quad (2)$$

at finite temperature. Note that the holographic contribution to the self-energy has both real and imaginary parts. Furthermore,  $0 < \nu < 1$  is the scaling dimension of the IR-CFT fermionic operator  $\chi$  which is related to the mass of the dual bulk fermion. The restriction on  $\nu$  is necessary in order for the holographic contribution to be relevant at low frequency. It is easy to check that the spectral function  $\rho = -2\text{Im}G$  is non-negative provided  $0 < \phi < \pi(1 - \nu)$  and  $\tilde{\alpha}, \tilde{\gamma} > 0$ .

Note in the high frequency or zero temperature limit  $\mathcal{G}(\omega, T)$  is  $e^{i\phi}\omega^\nu$  in agreement with the form studied in [32] at zero temperature. In the low energy limit  $\mathcal{G}(\omega, T) \approx T^\nu$ . Crucially the limit  $\nu \rightarrow 1$  yields a marginal Fermi liquid with a  $\omega \log \omega$  term in the self-energy and with a specific type of temperature dependence.

The model contains a single intrinsic scale, given by the Fermi energy  $E_F$ . It is useful to rewrite the propagator (1) in terms of dimensionless variables  $x := \omega/E_F$  and  $\mathbf{y} := \mathbf{k}/k_F$  in the form

$$G(x, \mathbf{y}) = E_F^{-1} \left( x + i\gamma(x^2 + (\pi x_T)^2) + \alpha e^{i(\phi + \pi\nu/2)} (2\pi x_T)^\nu \frac{\Gamma(\frac{1}{2} + \frac{\nu}{2} - i\frac{x}{2\pi x_T})}{\Gamma(\frac{1}{2} - \frac{\nu}{2} - i\frac{x}{2\pi x_T})} - (\mathbf{y}^2 - 1) \right)^{-1} \quad (3)$$

with  $x_T := T/E_F$ ,  $\alpha = \tilde{\alpha}E_F^{-(1-\nu)}$  and  $\gamma = \tilde{\gamma}E_F$ . Note  $\alpha$  and  $\gamma$  are dimensionless. Some plots of the spectral function are shown in Fig. 1.

The density-density correlation functions (the Lindhard function  $\mathcal{L}(q, \Omega)$ ) can be readily computed from the above spectral function at finite temperature. We reproduce the qualitative features of the zero temperature density-density correlations computed earlier in [32]. Even at finite temperatures  $T \approx 0.5E_F$ , the edges of the continuum are still prominent when  $\alpha, \gamma \ll 1$  although the response has sufficient support outside the continuum. Furthermore, there exist well-defined plasmonic excitations for  $q < 2.5k_F$  which have support inside the continuum when  $\approx 2k_F < q < \approx 2.5k_F$ . The dispersion relation of the plasmonic modes is approximately linear. (See Supplemental Material.) Furthermore, as noted in [32], it is important to consider  $1/2 < \nu \leq 1$  to avoid ultraviolet issues that destabilizes the infrared effective theory.

Finally we emphasize that it is necessary for  $\gamma$  to be sufficiently small and also  $\alpha < 1$  for the effective theory to be applicable at high frequencies and temperatures. If this is not the case, the effects of  $c$ -fermion running

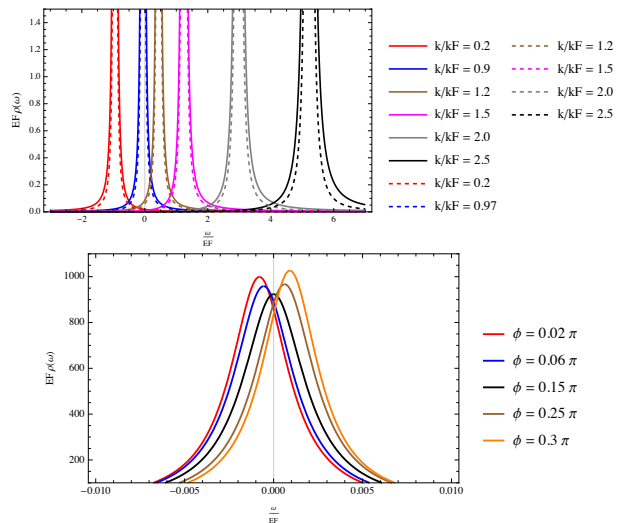


FIG. 1. TOP: The dimensionless spectral function  $E_F \rho(\omega)$  is plotted for various values of  $k/k_F$  at  $T = 0.5E_F$ ,  $\nu = 0.7$ ,  $\phi = 0.2\pi$  and  $\alpha = 0.016$  with the solid lines corresponding to  $\gamma = 0.001$  and the dashed lines corresponding to  $\gamma = 0$ . Note that the effects of non-vanishing  $\gamma$  is significant only for  $k$  away from  $k_F$ . BOTTOM: Here the dimensionless spectral function is plotted for  $T = 0.1E_F$ ,  $\nu = 0.7$ ,  $\gamma = 0.001$ ,  $\alpha = 0.016$  and various values of  $\phi$  between the allowed range 0 and  $(1 - \nu)\pi = 0.3\pi$  (see text) at  $k = k_F$ . Note that when  $\phi \approx 0.15\pi = \pi(1 - \nu)/2$ , the spectral function at the Fermi surface is nearly even in  $\omega$ .

in loops will spoil the separation of the self-energy into holographic and Fermi-liquid terms.

## DC CONDUCTIVITY

The DC conductivity can be computed readily from the simple formula

$$\sigma_{DC} \approx \frac{e^2}{2\hbar} \int \frac{d\omega}{2\pi} \int \frac{d^2k}{4\pi^2} k^2 \rho(\omega, \mathbf{k}, T)^2 \left( -\frac{\partial n_F(\omega, T)}{\partial \omega} \right) \quad (4)$$

Above  $n_F(\omega, T)$  denotes the Fermi-Dirac distribution function. Here we have used the exact bare vertices for the coupling with the photon and not simply its value on the Fermi surface which give the  $k^2$  term in the integrand.

It is quite easy to see that the low temperature behavior of the conductivity should be determined by the holographic critical sector so that  $\sigma_{DC}(T) \approx T^{-\nu}$  for  $T \ll 0.1E_F$ . For  $T > 0.1E_F$ , the Fermi liquid contribution to the self-energy is influential when  $0.001 \leq \gamma \leq 0.01$ . At high temperatures  $T \gg E_F$ , the DC conductivity becomes almost independent of the holographic critical sector and therefore does not depend on  $\alpha$ ,  $\nu$  and  $\phi$ . In this regime the scaling exponent decays rapidly implying that the rate of decay of the DC conductivity with temperatures slows down. We find that a scaling regime where  $\sigma_{DC} \approx T^{-\tilde{\nu}}$  with  $\tilde{\nu} \neq \nu$  and approximately

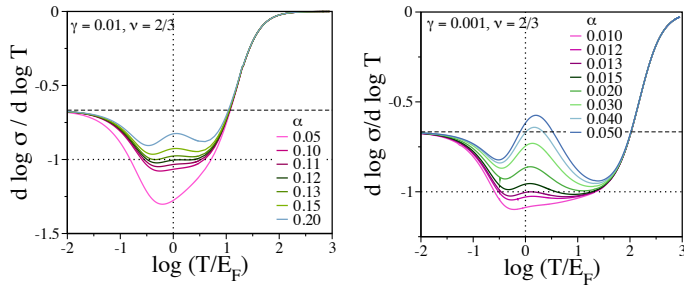


FIG. 2. The temperature dependence of the scaling of the conductivity with the temperature for  $\nu = 2/3$  is shown for various values of  $\alpha$  when  $\gamma = 0.01$  (on left) and  $\gamma = 0.001$  (on right). The upper horizontal dashed lines in both plots indicate that the scaling at very low  $T$  is  $-2/3$ . The linear scaling of resistivity appears in mid-temperature regime when  $\alpha \approx 13\gamma$ . At higher temperatures the conductivity is  $\alpha$  independent.

independent of the temperature emerges for  $\nu > \sim 0.67$  to a very good approximation at intermediate temperatures. Interestingly,  $\tilde{\nu} \approx 1$  implying linear-in- $T$  resistivity in this mid-temperature regime which stretches to arbitrary small values of temperatures when  $\nu$  approaches 1 where we obtain a marginal Fermi liquid with a specific temperature-dependent self energy. (Note we restrict ourselves to  $1/2 < \nu < 1$  for reasons mentioned above.)

Furthermore, we also find that the best approximation to the scaling in mid-temperature regime is obtained when the phase  $\phi$  in Eq. (1) takes its value around  $\pi(1 - \nu)/2$  (the mid-point of the allowed range of values). We therefore choose  $\phi$  to be around this value for the rest of this paper. We observe that in this case the spectral function at the Fermi surface is approximately even in  $\omega$  as shown in Fig. 1.

**Case 1 ( $0.5 < \nu < \sim 0.8$ ):** It is useful to first study the representative case of  $\nu = 2/3$  plotted in Fig. 2 where the independence of the high temperature behavior on the holographic sector is manifest. In the intermediate temperature regime, the scaling exponent  $d \log \sigma_{DC} / d \log T$  is non-monotonic. However, crucially we observe that when  $\alpha \approx 13\gamma$ , there is a scaling regime in which the scaling exponent is temperature independent for both  $\gamma = 0.01$  and  $\gamma = 0.001$  and furthermore it is approximately  $-1$  implying linear-in- $T$  resistivity. Remarkably, the range of temperatures where this occurs is quite wide extending from about  $0.3E_F$  to nearly  $10E_F$  when  $\gamma = 0.01$  and nearly  $20E_F$  when  $\gamma = 0.001$ .

Such a scaling regime at intermediate temperature regime does not arise for  $\nu < \sim 0.67$ . In Fig. 3, we report the dependence of the scaling exponent on the temperature at various values of  $\nu$  ranging between 0.5 and 1 for  $\gamma = 0.001$  and for those values of  $\alpha$  where we get the best approximation to linear scaling of the DC resistivity with the temperature. Clearly, for  $\nu = 0.55$ , there

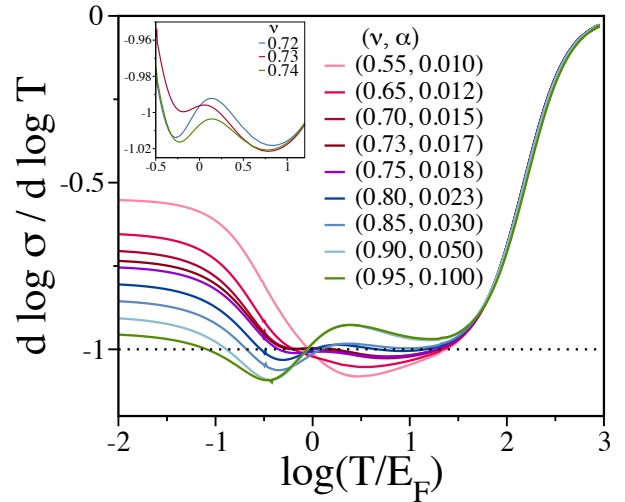


FIG. 3. The scaling exponent of the DC conductivity is plotted for various values of  $\nu$  between 0.5 and 1 at  $\gamma = 0.001$ . Above  $\alpha$  has been chosen for each  $\nu$  such that the best approximation to linear-in- $T$  resistivity is obtained in the mid-temperature regime. The inset plot shows that the best linear-in- $T$  scaling is obtained for  $\nu = 0.73, \alpha = 0.017$ . At higher temperature the conductivity is almost independent of holographic effects, i.e.  $\nu$  and  $\alpha$ .

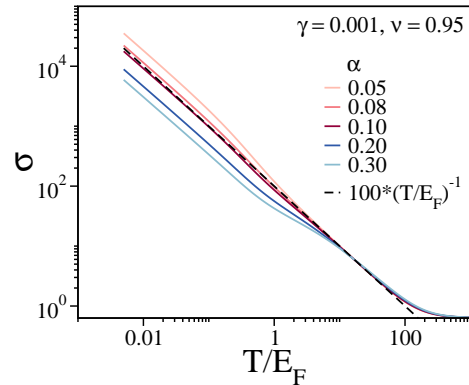


FIG. 4. The temperature dependence of the DC conductivity is plotted above for  $\nu = 0.95, \gamma = 0.001$  and various values of  $\alpha$ . The best approximation to linear-in- $T$  resistivity is obtained for  $\alpha = 0.1$ . The scaling exponent for this case has been plotted as a function of the temperature in Fig 3.

is no scaling regime for  $T > 0.1E_F$ . The best approximation to the linear-in- $T$  resistivity in the temperature range that includes  $E_F$  is obtained when  $\nu = 0.73$  and  $\alpha = 0.017$  (see inset plot of Fig 3 where it shows that the scaling exponent varies between 0.98 and 1.02 for  $0.3E_F < T < 30E_F$ ).

Thus we obtain linear-in- $T$  resistivity to a remarkable approximation in the mid-temperature regime  $T_{min} < T < T_{max}$  with  $E_F$  included in this range for  $\sim 0.67 < \nu < \sim 0.8$  if we choose the optimal ratio  $\alpha/\gamma$  for each  $\nu$  while setting  $\phi$  near  $\pi(1 - \nu)/2$  as mentioned above. The

higher end of this scaling regime ( $T_{max}$ ) strongly depends on  $\gamma$  but the lower end ( $T_{min}$ ) depends only mildly on  $\gamma$  and the parameters of the holographic sector.

**Case 2** ( $\sim 0.8 < \nu \leq 1$ ): For higher values of  $\nu$  we can still obtain the linear-in-T resistivity in the mid-temperature regime including  $T \approx E_F$  by tuning  $\alpha/\gamma$  for each choice of  $\nu$  as shown in Fig. 3. However, the scaling is less accurate, i.e.  $-1 \pm 0.1$  percent instead of  $-1 \pm 0.05$ . In the case of  $\nu = 0.85$ , as for instance, we get an excellent linear-in-T resistivity only at higher range of temperatures between  $3E_F$  and  $30E_F$ . However, if we allow for 10 percent variation of the scaling exponent, then the scaling regime stretches to arbitrarily low temperatures as illustrated in the case of  $\nu = 0.95$  in Fig. 4. This continues to hold as we approach the marginal Fermi liquid  $\nu \approx 1$ .

## DISCUSSION

We have shown that in our effective semi-holographic approach which shares common features with Mottness, the linear-in-T resistivity emerges for a very wide range of temperatures irrespectively of the holographic critical sector provided  $\nu > \sim 0.67$  and we tune the ratio of the two couplings optimally. Although the Fermi energy provides the unique energy scale of our model, in order to match it with a material we should probably use a lower

energy scale in practice, such as a crossover scale where Fermi liquid effects are dominant. In any case the model is just the first step to a more viable theory that can be applied to real-world strange metals.

It is useful to compare our approach to some recently discussed models involving a lattice of (complex) SYK quantum dots exchanging fermions via hopping [36–42] which also can reproduce linear-in-T resistivity (see also [43]). A heuristic connection with our approach readily emerges from the observation that (nearly)  $AdS_2$  holography can capture many aspects of SYK systems [44]. Thus a lattice of  $AdS_2$  throats representing a fragmented  $AdS_2 \times R^2$  geometry recently proposed as a model for quantum black hole microstates [45] could be actually also relevant for our approach. Aided via DMFT methods in which the Anderson impurity atom is replaced by a single  $AdS_2$  throat, we aim to understand the thermodynamic reason for why a certain ratio of the couplings can be preferred. We also plan to explore magneto-transport and the superconducting instability.

It is a pleasure to thank Johanna Erdmenger, Rene Meyer, Ronny Thomale, Mukul Laad and Shantanu Mukherjee for helpful discussions. AM acknowledges support from the Ramanujan Fellowship and ECR award of the Department of Science and Technology of India. AM and GP also acknowledge generous support from IFCPAR/CEFIPRA funded project no 6403.

## SUPPLEMENTAL MATERIAL: THE GENERALIZED LINDHARD FUNCTION AND THE PLASMONIC EXCITATIONS

The density-density response function  $\mathcal{L}$  (generalized Lindhard function) is schematically

$$\mathcal{L}(\Omega, q) = -2i \int_k \int_\omega G(\omega_+, \mathbf{k}_+) G(\omega_-, \mathbf{k}_-), \quad (5)$$

where  $\omega_\pm = \omega \pm \Omega/2$  and  $\mathbf{k}_\pm = \mathbf{k} \pm q/2$ . In terms of the variables introduced in the main text, the imaginary part of the Lindhard function explicitly is

$$\begin{aligned} \text{Im}\mathcal{L}(x_\Omega, y_q, x_T) &= 4 \int_{-\infty}^{\infty} dx \int d^2y \text{Im}G\left(x + \frac{x_\Omega}{2}, y + \frac{y_q}{2}, x_T\right) \\ &\quad \text{Im}G\left(x - \frac{x_\Omega}{2}, y - \frac{y_q}{2}, x_T\right) \\ &\quad \left(n_F\left(x + \frac{x_\Omega}{2}, x_T\right) - n_F\left(x - \frac{x_\Omega}{2}, x_T\right)\right) \end{aligned} \quad (6)$$

The plot of  $\text{Im}\mathcal{L}$  as a function of  $x_\Omega$  is shown in Fig. 5. The continuum extends between  $0 < \Omega < q^2/2m + 2qk_F/m$ , i.e. between  $0 < x_\Omega < y_q^2 + 2y_q$  for  $q \leq 2k_F$  (i.e.  $y_q \leq 2$ ) and between  $q^2/2m - 2qk_F/m < \Omega < q^2/2m + 2qk_F/m$ , i.e. between  $y_q^2 - 2y_q < x_\Omega < y_q^2 + 2y_q$  for  $q > 2k_F$  (i.e.  $y_q > 2$ ). As for instance, for  $y_q = 1$ , the maximum support is in the region  $0 < x_\Omega < 3$  and for  $y_q = 3$  the range of maximum support is  $3 < x_\Omega < 15$ . It is clear from Fig. 5 that  $\text{Im}\mathcal{L}$  is supported maximally within the continuum although the edges are blurred out especially for higher values of  $q$ .

We compute the real part of the Lindhard function using the Kramers-Krönig relation:

$$\text{Re}\mathcal{L}(x_\Omega) = \lim_{\epsilon \rightarrow 0} \frac{1}{\pi} \int_0^\infty dx \text{Im}\mathcal{L}(x) \left( \frac{x - x_\Omega}{(x - x_\Omega)^2 + \epsilon^2} + \frac{x + x_\Omega}{(x + x_\Omega)^2 + \epsilon^2} \right). \quad (7)$$

We put a cut-off on the  $x$ -integral at  $x = 30$  and set  $\epsilon = 10^{-4}$  while evaluating the above integral numerically. The plot of  $\text{Re}\mathcal{L}$  is shown in Fig. 6.

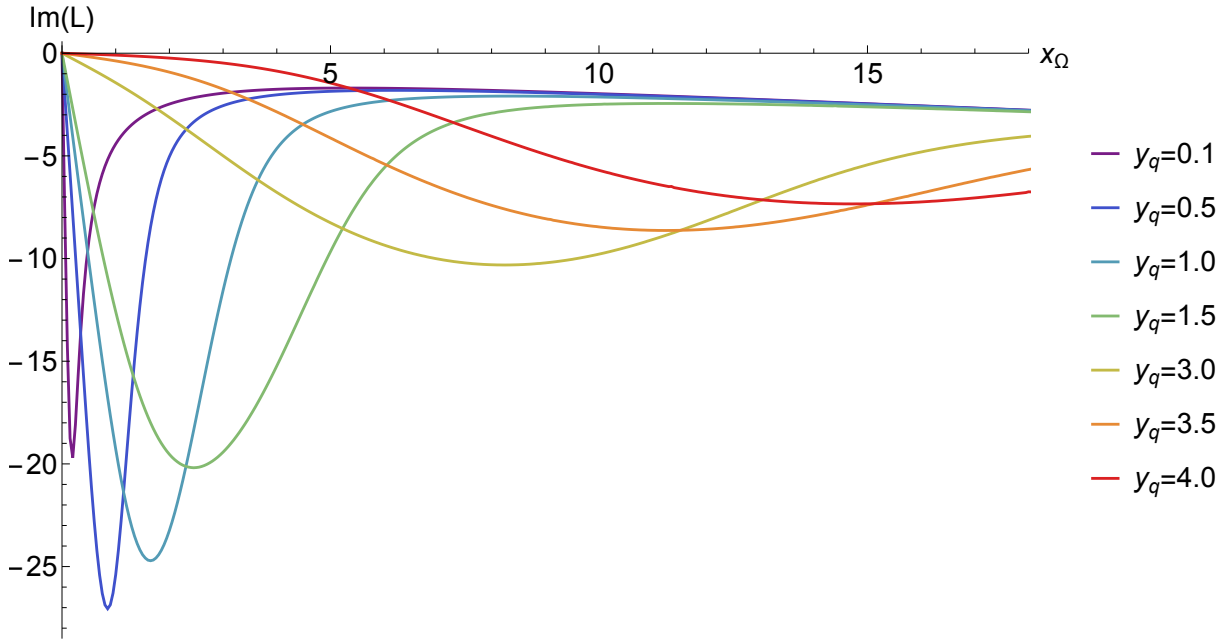


FIG. 5. Imaginary part of the Lindhard function as a function of  $x_\Omega$ . We have set  $x_T = 0.5$ ,  $\alpha = 0.12$  and  $\gamma = 0.01$ .

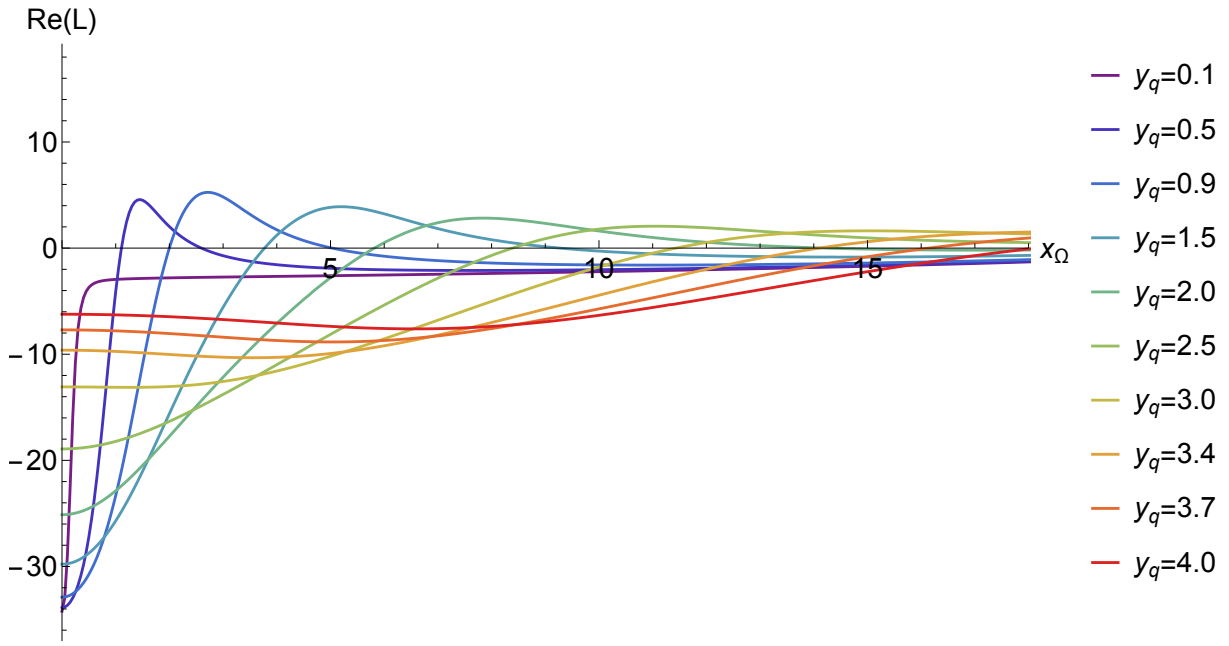


FIG. 6. Real part of the Lindhard function as a function of  $x_\Omega$ . We have set  $x_T = 0.5$ ,  $\alpha = 0.12$  and  $\gamma = 0.01$ .

The bubble resummation produces the improved generalized Lindhard function which is given by

$$\mathcal{L}^{\text{imp}}(x_\Omega, y_q, x_T) = \frac{\mathcal{L}(x_\Omega, y_q, x_T)}{1 - V(y_q)\mathcal{L}(x_\Omega, y_q, x_T)}, \quad (8)$$

where  $V(y_q)$  is the Coulomb potential. In 2D, this is inversely proportional to  $y_q$ . The real and imaginary parts of the improved Lindhard function are shown in Fig. 7. Fig. 8 shows the contour plot for imaginary part of the improved Lindhard function. In these figures we have chosen the values of the couplings and the temperature such that they lie in the regime of linear  $T$  resistivity. The well defined plasmonic poles with linear dispersion relation are prominently visible. Around  $q = 2k_F$ , the plasmonic excitations have sufficient support inside the continuum which could not have

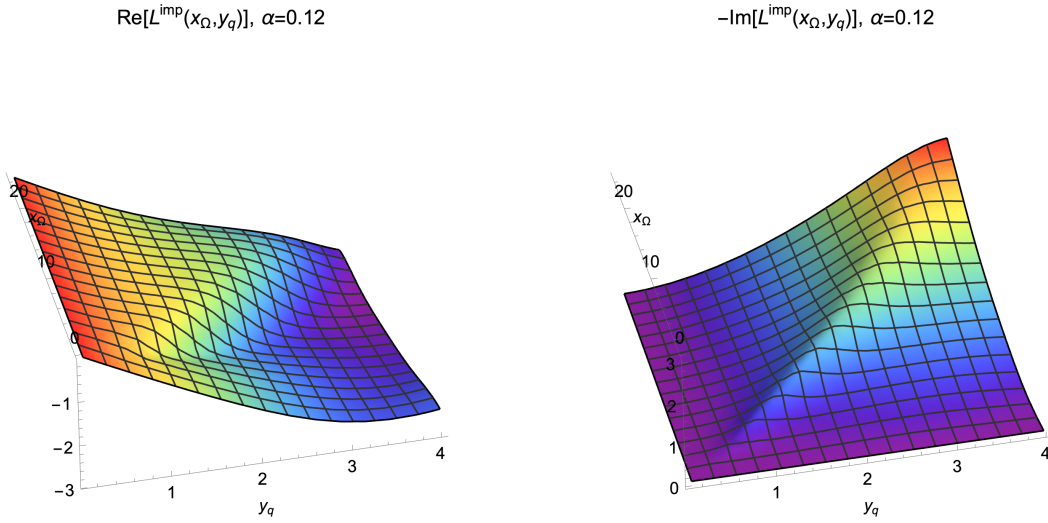


FIG. 7. Real and imaginary part of the improved Lindhard function as a function of  $x_\Omega$  and  $y_q$  when  $x_T = 0.5$ . We have set  $\alpha = 0.12$  and  $\gamma = 0.01$ .

occurred in the case of a Fermi liquid.

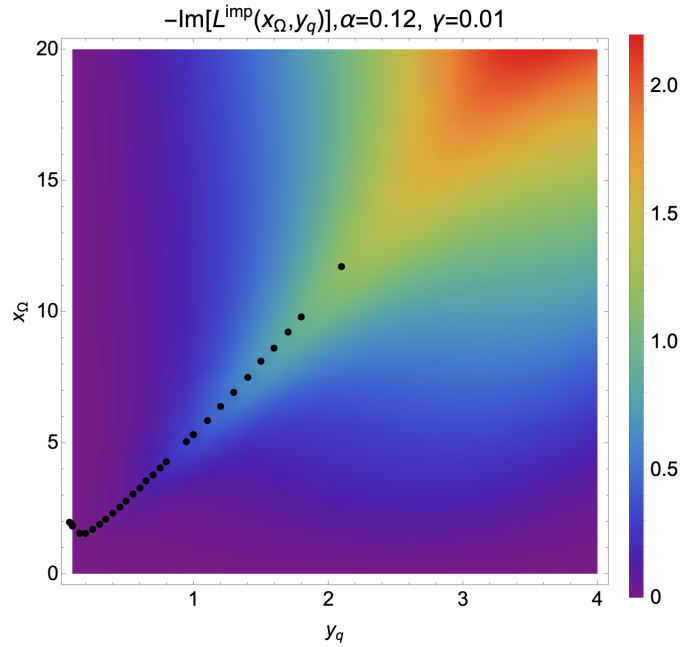


FIG. 8. Density plot of imaginary part of the improved Lindhard function with the maxima shown as the black dots. We have set  $x_T = 0.5$ ,  $\alpha = 0.12$  and  $\gamma = 0.01$ .

---

\* doucot@lpthe.jussieu.fr  
 † ayan@physics.iitm.ac.in  
 ‡ policast@lpt.ens.fr

<sup>§</sup> psss2238@iacs.res.in

- [1] Andrea Damascelli, Zahid Hussain, and Zhi-Xun Shen, “Angle-resolved photoemission studies of the cuprate superconductors,” *Rev. Mod. Phys.* **75**, 473–541 (2003).
- [2] I M Vishik, W S Lee, R-H He, M Hashimoto, Z Hussain, T P Devereaux, and Z-X Shen, “ARPES studies of cuprate fermiology: superconductivity, pseudogap and quasiparticle dynamics,” *New Journal of Physics* **12**, 105008 (2010).
- [3] T. J. Reber, X. Zhou, N. C. Plumb, S. Parham, J. A. Waugh, Y. Cao, Z. Sun, H. Li, Q. Wang, J. S. Wen, Z. J. Xu, G. Gu, Y. Yoshida, H. Eisaki, G. B. Arnold, and D. S. Dessau, “Power law liquid - a unified form of low-energy nodal electronic interactions in hole doped cuprate superconductors,” (2015), arXiv:1509.01611 [cond-mat.str-el].
- [4] T. Senthil, “Critical fermi surfaces and non-fermi liquid metals,” *Phys. Rev. B* **78**, 035103 (2008).
- [5] Sung-Sik Lee, “Recent developments in non-fermi liquid theory,” *Annual Review of Condensed Matter Physics* **9**, 227–244 (2018).
- [6] Chandra M. Varma, “Colloquium: Linear in temperature resistivity and associated mysteries including high temperature superconductivity,” *Rev. Mod. Phys.* **92**, 031001 (2020).
- [7] Sung-Sik Lee, “A Non-Fermi Liquid from a Charged Black Hole: A Critical Fermi Ball,” *Phys. Rev. D* **79**, 086006 (2009), arXiv:0809.3402 [hep-th].
- [8] Hong Liu, John McGreevy, and David Vegh, “Non-Fermi liquids from holography,” *Phys. Rev. D* **83**, 065029 (2011), arXiv:0903.2477 [hep-th].
- [9] Mihailo Cubrovic, Jan Zaanen, and Koenraad Schalm, “String Theory, Quantum Phase Transitions and the Emergent Fermi-Liquid,” *Science* **325**, 439–444 (2009), arXiv:0904.1993 [hep-th].
- [10] Thomas Faulkner, Hong Liu, John McGreevy, and David Vegh, “Emergent quantum criticality, Fermi surfaces, and AdS(2),” *Phys. Rev. D* **83**, 125002 (2011), arXiv:0907.2694 [hep-th].
- [11] Thomas Faulkner, Nabil Iqbal, Hong Liu, John McGreevy, and David Vegh, “From Black Holes to Strange Metals,” (2010), arXiv:1003.1728 [hep-th].
- [12] Nabil Iqbal, Hong Liu, and Mark Mezei, “Semi-local quantum liquids,” *JHEP* **04**, 086 (2012), arXiv:1105.4621 [hep-th].
- [13] T. Senthil, Ashvin Vishwanath, Leon Balents, Subir Sachdev, and Matthew P.A. Fisher, “Deconfined Quantum Critical Points,” *Science* **303**, 1490–1494 (2004), arXiv:cond-mat/0311326.
- [14] Sean A. Hartnoll, Andrew Lucas, and Subir Sachdev, “Holographic quantum matter,” (2016), arXiv:1612.07324 [hep-th].
- [15] Philip Phillips, “Mottness,” *Annals of Physics* **321**, 1634 – 1650 (2006), July 2006 Special Issue.
- [16] Ting-Pong Choy, Robert G. Leigh, Philip Phillips, and Philip D. Powell, “Exact integration of the high energy scale in doped mott insulators,” *Phys. Rev. B* **77**, 014512 (2008).
- [17] Shiro Sakai, Yukitoshi Motome, and Masatoshi Imada, “Evolution of electronic structure of doped mott insulators: Reconstruction of poles and zeros of green’s function,” *Phys. Rev. Lett.* **102**, 056404 (2009).
- [18] Youhei Yamaji and Masatoshi Imada, “Composite-fermion theory for pseudogap, fermi arc, hole pocket, and non-fermi liquid of underdoped cuprate superconductors,” *Phys. Rev. Lett.* **106**, 016404 (2011).
- [19] Youhei Yamaji and Masatoshi Imada, “Composite fermion theory for pseudogap phenomena and superconductivity in underdoped cuprate superconductors,” *Phys. Rev. B* **83**, 214522 (2011).
- [20] Seungmin Hong and Philip Phillips, “Towards the standard model for fermi arcs from a wilsonian reduction of the hubbard model,” *Phys. Rev. B* **86**, 115118 (2012).
- [21] Steven S. Gubser and Fabio D. Rocha, “Peculiar properties of a charged dilatonic black hole in  $AdS_5$ ,” *Phys. Rev. D* **81**, 046001 (2010), arXiv:0911.2898 [hep-th].
- [22] Sean A. Hartnoll, Joseph Polchinski, Eva Silverstein, and David Tong, “Towards strange metallic holography,” *JHEP* **04**, 120 (2010), arXiv:0912.1061 [hep-th].
- [23] Christos Charmousis, Blaise Gouteraux, Bom Soo Kim, Elias Kiritsis, and Rene Meyer, “Effective Holographic Theories for low-temperature condensed matter systems,” *JHEP* **11**, 151 (2010), arXiv:1005.4690 [hep-th].
- [24] Thomas Faulkner, Nabil Iqbal, Hong Liu, John McGreevy, and David Vegh, “Strange metal transport realized by gauge/gravity duality,” *Science* **329**, 1043–1047 (2010).
- [25] Bum-Hoon Lee, Da-Wei Pang, and Chanyong Park, “Strange Metallic Behavior in Anisotropic Background,” *JHEP* **07**, 057 (2010), arXiv:1006.1719 [hep-th].
- [26] Richard A. Davison, Koenraad Schalm, and Jan Zaanen, “Holographic duality and the resistivity of strange metals,” *Phys. Rev. B* **89**, 245116 (2014), arXiv:1311.2451 [hep-th].
- [27] Zhenhua Zhou, Jian-Pin Wu, and Yi Ling, “DC and Hall conductivity in holographic massive Einstein-Maxwell-Dilaton gravity,” *JHEP* **08**, 067 (2015), arXiv:1504.00535 [hep-th].
- [28] Sera Cremonini, Anthony Hoover, Li Li, and Steven Waskie, “Anomalous scalings of cuprate strange metals from nonlinear electrodynamics,” *Phys. Rev. D* **99**, 061901 (2019), arXiv:1812.01040 [hep-th].
- [29] Hyun-Sik Jeong, Keun-Young Kim, and Chao Niu, “Linear- $T$  resistivity at high temperature,” *JHEP* **10**, 191 (2018), arXiv:1806.07739 [hep-th].
- [30] Thomas Faulkner and Joseph Polchinski, “Semi-Holographic Fermi Liquids,” *JHEP* **06**, 012 (2011), arXiv:1001.5049 [hep-th].
- [31] Ayan Mukhopadhyay and Giuseppe Policastro, “Phenomenological Characterization of Semiholographic Non-Fermi Liquids,” *Phys. Rev. Lett.* **111**, 221602 (2013), arXiv:1306.3941 [hep-th].
- [32] Benoit Doucot, Christian Ecker, Ayan Mukhopadhyay, and Giuseppe Policastro, “Density response and collective modes of semiholographic non-Fermi liquids,” *Phys. Rev. D* **96**, 106011 (2017), arXiv:1706.04975 [hep-th].
- [33] A. J. Leggett, “A “midinfrared” scenario for cuprate superconductivity,” *Proceedings of the National Academy of Sciences* **96**, 8365–8372 (1999), <https://www.pnas.org/content/96/15/8365.full.pdf>.



- [34] Anthony J. Leggett, “What do we know about high  $t_c$ ?” *Nature Physics* **2**, 134–136 (2006).
- [35] Nabil Iqbal and Hong Liu, “Real-time response in AdS/CFT with application to spinors,” *Fortsch. Phys.* **57**, 367–384 (2009), arXiv:0903.2596 [hep-th].
- [36] Xue-Yang Song, Chao-Ming Jian, and Leon Balents, “Strongly correlated metal built from sachdev-ye-kitaev models,” *Phys. Rev. Lett.* **119**, 216601 (2017).
- [37] Aavishkar A. Patel, John McGreevy, Daniel P. Arovas, and Subir Sachdev, “Magnetotransport in a model of a disordered strange metal,” *Phys. Rev. X* **8**, 021049 (2018).
- [38] Debanjan Chowdhury, Yochai Werman, Erez Berg, and T. Senthil, “Translationally invariant non-fermi-liquid metals with critical fermi surfaces: Solvable models,” *Phys. Rev. X* **8**, 031024 (2018).
- [39] Aavishkar A. Patel, Michael J. Lawler, and Eun-Ah Kim, “Coherent superconductivity with a large gap ratio from incoherent metals,” *Phys. Rev. Lett.* **121**, 187001 (2018).
- [40] Peter Cha, Nils Wentzell, Olivier Parcollet, Antoine Georges, and Eun-Ah Kim, “Linear resistivity and sachdev-ye-kitaev (syk) spin liquid behavior in a quantum critical metal with spin-1/2 fermions,” *Proceedings of the National Academy of Sciences* **117**, 18341–18346 (2020).
- [41] Connie H. Mousatov, Ilya Esterlis, and Sean A. Hartnoll, “Bad metallic transport in a modified hubbard model,” *Phys. Rev. Lett.* **122**, 186601 (2019).
- [42] Aavishkar A. Patel and Subir Sachdev, “Theory of a planckian metal,” *Phys. Rev. Lett.* **123**, 066601 (2019).
- [43] Peter Cha, Aavishkar A. Patel, Emanuel Gull, and Eun-Ah Kim, “Slope invariant  $t$ -linear resistivity from local self-energy,” *Phys. Rev. Research* **2**, 033434 (2020).
- [44] Gábor Sárosi, “AdS<sub>2</sub> holography and the SYK model,” *PoS Modave2017*, 001 (2018), arXiv:1711.08482 [hep-th].
- [45] Tanay Kibe, Ayan Mukhopadhyay, Alexander Soloviev, and Hareram Swain, “ $SL(2, R)$  lattices as information processors,” *Phys. Rev. D* **102**, 086008 (2020), arXiv:2006.08644 [hep-th].